Spin-asymmetry function for elastic electron scattering from lead atoms in the energy range 11–14 eV

V. Hamelbeck* and G. F. Hanne†
Physikalisches Institut, Universität Münster, Wilhelm-Klemm-Str. 10, 48149 Münster, Germany

O. Zatsarinny and K. Bartschat‡
Department of Physics and Astronomy, Drake University, Des Moines, Iowa 50311, USA

R. K. Gangwar and R. Srivastava§
Department of Physics, Indian Institute of Technology Roorkee, Roorkee 247667, India
(Received 23 September 2009; published 7 December 2009)

We report investigations of the spin-asymmetry function S_A in elastic electron scattering from lead atoms. The experimental results are compared to previous measurements as well as to earlier and recent relativistic model-potential and *R*-matrix (close-coupling) calculations. The spin-asymmetry function is found to depend strongly on the incident-electron energy in the region between 11 and 14 eV.

DOI: 10.1103/PhysRevA.80.062711 PACS number(s): 34.80.Nz, 34.80.Bm

I. INTRODUCTION

Observing spin effects in electron-atom collisions often provides a deeper insight into the dynamics of scattering processes than spin-averaged measurements [1–3]. In particular, collision experiments with heavy open-shell atoms and spin-polarized electron beams are performed to study the simultaneous occurrence of spin-orbit and electron exchange effects. Describing these processes accurately for complex atoms is still a formidable challenge for state-of-the-art theory.

Many investigations have been carried out using lead (Pb) as a target in electron-atom collisions. For low energies down to 0.3 eV, the results of Dummler *et al.* [4] show good agreement with predictions from *R*-matrix (close-coupling) calculations that include both Mott scattering and the "fine-structure effect" [5], i.e., a spin dependence of the collision process caused by angular-momentum orientation in combination with resolving individual members of a fine-structure multiplet with fixed total electronic angular momentum *J*. Kaussen *et al.* [6] investigated the spin polarization after elastic scattering of unpolarized electrons from several heavy atoms, including lead, for selected incident-electron energies between 6 and 180 eV. Later, Geesmann *et al.* [7] used a source of spin-polarized electrons to study the spin-asymmetry function for incident energies ranging between 2.5 and 14 eV and scattering angles in the range 35–125°. Based on these measurements and generalized Kohn-Sham (GKS) calculations by Haberland and Fritsche [8] presented by Geesmann *et al.*, it was concluded that for elastic e-Pb scattering the "fine-structure effect" only has a small influence for collision energies down to 6 eV.

For 11 eV, Geesmann *et al.* [7] noted significant discrepancies between the predictions from the GKS theory and their experimental data. Furthermore, the angular dependence of the spin-asymmetry function S_A exhibited a significant change when changing the energy from 11 to 14 eV. Hence, we revived these experiments to investigate this particular energy range between 11 and 14 eV incident energy in more detail. Because of the strong energy dependence special care was given to ensure an accurate energy calibration.

The structure of this paper is as follows. In Sec. II, the physics of the spin-asymmetry function is briefly reviewed and a summary of the computational methods employed for the numerical calculations is given. Two different numerical methods have been applied, namely a relativistic model-potential (RMP) method, which is a one-channel approach with the addition of semiempirical local potentials, and a fully *ab initio* nonperturbative *R*-matrix (close-coupling) approach, in which these effects are represented through coupling to other states. The experimental setup and some details of the measurements are summarized in Sec. III, before the results are presented and discussed in Sec. IV. Finally, some conclusions are drawn and an outlook is given for future work in this area.

II. THEORETICAL BACKGROUND

We begin this section by briefly explaining in Sec. II A the physical meaning of the spin-asymmetry function as the observable of interest for the present work. This is followed by summaries of the numerical methods used to calculate this parameter, starting with the fully RMP approach (IIB) and followed by two *R*-matrix (close-coupling) models (IIC).

A. Spin-asymmetry function

The spin-asymmetry function S_A is a measure for the spin dependence of the differential cross section (DCS) in collisions of spin-polarized electrons with a given target. An illustration of the polarization dependent scattering intensities is shown in Fig. 1. For the so-called "Mott scattering" a simple picture can be given as follows. From the point of view of the incident electron approaching the atomic

*volker.hamelbeck@uni-muenster.de
†hanne@uni-muenster.de
‡klaus.bartschat@drake.edu
§rajsrfph@gmail.com

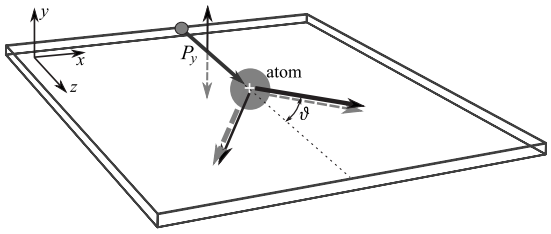

FIG. 1. Illustration of the spin-dependent scattering intensities in the so-called *collision frame*, in which the incident-beam direction defines the quantization (z) axis. We show the two cases of either primary spin-up (black solid, ↑) or spin-down (gray dashed, ↓) polarization P_y perpendicular to the xz collision plane. The thickness of the lines corresponds to the particular scattering intensities $N^{\uparrow}$ and $N^{\downarrow}$, respectively.

nucleus, the relative orbital motion evokes a magnetic field, which then interacts with the spin magnetic moment of the electron. Hence, the interaction potential directly depends on the incident spin orientation. The spin dependence of the DCS leads to different scattering intensities for a fixed angle ϑ if a spin-polarized electron beam is used.

If $N^{\uparrow}(\vartheta)$ and $N^{\downarrow}(\vartheta)$ are the detected count rates of electrons with initial spin-up and spin-down polarization P_y, respectively, the spin-asymmetry function S_A is given by [9]

$$S_A(\vartheta) = \frac{1}{P_y} \cdot \frac{N^{\uparrow}(\vartheta) - N^{\downarrow}(\vartheta)}{N^{\uparrow}(\vartheta) + N^{\downarrow}(\vartheta)}. \quad (1)$$

For symmetry reasons $N^{\uparrow}(\vartheta)=N^{\downarrow}(-\vartheta)$ so that S_A also describes the left-right asymmetry of spin-polarized electron scattering.

The mechanism for the "fine-structure effect" [5] is different from "Mott scattering." In this case, selecting a particular fine-structure level from a multiplet may lead to different probabilities for exchange between the projectile and a target electron if the orbital angular momentum of the target becomes oriented through the collision process. Details can be found in Ref. [5], but it is worth mentioning that the strength of the spin dependence is only relevant from the experimental point of view regarding the ability to resolve the fine-structure level. Hence, the physics of this effect is essentially independent of the nuclear charge and is most clearly observed in light targets and at smaller scattering angles, where effects due to Mott scattering are generally small.

B. Relativistic model-potential calculations

An effective optical model-potential approach along with solving the Dirac equation was recently used to study the elastic scattering of electrons from Pb atoms. The calculated angle-differential and angle-integrated cross sections were found to be in excellent agreement with the reported experimental data [10]. Employing the same approach, we performed two RMP calculations for the spin-asymmetry function S_A for the present paper. These calculations differed in the wave functions used for the target description.

In our RMP approach, the motion of the projectile electron in a central field $V(r)$ is described by the Dirac equation, which is solved using a partial-wave phase-shift analysis [10]. The required total interaction potential $V(r)$ between the projectile electron and the target atom is approximately represented by an effective complex model potential. The real part of the potential was chosen to be the sum of three local terms, namely the static (V_{st}), exchange (V_{ex}), and polarization (V_{pol}) potentials. These terms are functions of the electronic charge density of the target and approximately account for the dynamics of the collisional process. The static potential $V_{st}(r)$ and the charge density $\rho(r)$ are calculated from relativistic Dirac-Fock wave functions that were obtained from the GRASP92 code of Parpia *et al.* [11]. Since Hartree-Fock wave functions [12] were used in most earlier calculations [10], we also considered those in the present calculation. For the exchange potential V_{ex}, a modified semiclassical exchange potential as given by Gianturco and Sciallia [13] was employed. Finally, in order to account for all the inelastic process during the scattering, we used a modified version of the semiempirical absorption potential of Staszewska *et al.* [10,14].

Since we are interested in the low-energy region for this paper, a different polarization potential was taken from that used in ref. [10] as the same polarization potential was found not adequate to describe the backward scattering. In fact, the slow projectile causes a strong polarization of the charge cloud in the target atom and, in turn, the induced dipole moment acts back on the projectile. Several forms for (V_{pol}) are available in the literature, which have been tested for elastic electron scattering from the ground state of various atoms. The calculations performed here used a simple form of V_{pol} that has proven to produce good results for the elastic scattering of electrons atoms in their ground state [15–17]. Specifically, the potential has two components, one for the short range, $r<r_c$, of the Buckingham-type polarization potential [15] and another for the long range, $r \geq r_c$. The long-range form of the polarization potential was as usual taken as $V_{pol}=-\alpha_d/2r^4$, where α_d is the static electric-dipole polarizability of the lead atom in its $^3P_0$ ground state [10]. The radius r_c is the point where the two forms of the polarization potential switch over. In the short-range part of the polarization potential, the energy dependent β parameter [15] and r_c are chosen such that these provide the best shape fitting to the experimental spin-asymmetry function at a particular energy. Our values of β vary in the range of 1.25–1.55 for incident-electron energies between 11 to 14 eV and r_c was taken to be 5.0. As mentioned earlier, we used the relativistic Dirac-Fock (DF) wave function obtained from the GRASP92 code of Parpia *et al.* [11] and the Hartree-Fock (HF) wave function [12] that was frequently used in earlier elastic-scattering calculations. These two calculations are referred to as RMP-DF and RMP-HF, respectively.

C. *R*-matrix calculations

We also performed two *R*-matrix (close-coupling) calculations using (i) a five-state semirelativistic Breit-Pauli (BPRM-5cc) and (ii) a 20-state fully relativistic Dirac *B*-spline *R*-matrix (DBSR-20cc) approach.

The BPRM-5cc model was described by Bartschat [18]. It closely couples the five states with dominant configuration

$(6s^2 6p^2)$, i.e., $^3P_{0,1,2}$, $^1D_2$, and $^1S_0$. The one-electron orbitals were calculated with the program SUPERSTRUCTURE of Eissner *et al.* [19]. The target was actually treated as a quasi-two-electron system, i.e., the inner 80 electrons up to the filled $6s$ subshell were represented by the statistical model potential generated by SUPERSTRUCTURE. Relativistic effects were accounted for at the level of the one-electron terms in the Breit-Pauli hamiltonian, i.e., the spin-orbit interaction, mass correction, and Darwin terms. The Belfast suite of *R*-matrix codes, RMATRX-I, of Berrington *et al.* [20] was used to solve the problem in the inner region, and the asymptotic program FARM [21] was employed to obtain the transition-matrix elements. Finally, the program MJK of Grum-Grzhimailo [22] was employed to calculate the scattering amplitudes and the spin-asymmetry function S_A.

One would generally not expect the BPRM-5cc model to be appropriate for the problem of interest, due to the approximate treatment of relativistic effects for this very heavy target and the lack of coupling to other states, especially those that can be reached via optically allowed transitions and thus account for the dipole polarizability of the initial state. Indeed, this approach did not perform very well when its predictions were compared to previous experimental data for the e-Pb collision system [7], in particular for inelastic transitions.

A highly successful modification of the standard *R*-matrix approach, developed over the past decade, has been the *B*-spline *R*-matrix (BSR) method of Zatsarinny and coworkers. A detailed description of the method, the computer program, and many references to early applications can be found in the write-up by Zatsarinny [23]. Of particular interest for the current work is the recent extension of the approach to a fully relativistic Dirac-Coulomb framework [24], with subsequent successful applications to electron collisions with Au [25,26] and Hg [27,28].

The Dirac-based *B*-spline *R*-matrix (DBSR) approach is based on the same idea as the Breit-Pauli version described in [23]. The key points are (i) the use of basis (*B*-) splines as the underlying, effectively complete basis to expand the one-electron orbitals (spinors) of both the valence electrons and the projectile and (ii) the possibility to use individually optimized, term-dependent, and hence nonorthogonal orbitals to improve the target description substantially over what would be possible with a small set of configurations constructed from orthogonal orbitals. For the present problem, we generated 20 target states with the dominant configurations $6s^2 6p^2$ (the same five states as in the BPRM-5cc model described above), $6p^4$ (another five states), and $6s6p^3$ (a total of ten states). All these states were obtained with the relativistic structure code GRASP2K [29], at the level of the single-configuration Dirac-Fock approximation. Specifically, we used the same set of configuration-averaged $6s$ and $6p$ spinors for the even-parity states but a different set for the odd-parity $6s6p^3$ states.

Note that the latter states are not only strongly connected to the ground state via the optically $6s \rightarrow 6p$ one-electron transition, but several of them lie in the autoionizing region between 11 and 14 eV above the ground state that is of interest for the present work. Hence, including these states in the close-coupling expansion is likely to be important for accurate theoretical predictions to be produced in an *ab initio* model. This was the principal reason for including these states rather than additional valence states with configurations $6s^2 6pnl$. In fact, test calculations with a number of such states but without the $6s6p^3$ states produced very similar results to those obtained in the BPRM-5cc model.

While it would be desirable to generate even more states in a term-dependent multiconfiguration framework and to include them in the close-coupling expansion to obtain fully converged results, this is a very challenging problem and goes far beyond the scope of the present work. Nevertheless, as will be seen below, the above DBSR-20cc model goes a long way to reproduce the current experimental data. As a final detail, we used 111 *B*-splines of order 8 and 9 for the large and small components of the orbitals, respectively, to span the internal *R*-matrix region up to the box radius of $50a_0$, where $a_0 = 0.529 \times 10^{-10}$ m is the Bohr radius. Summing contributions up to $J = 41/2$ of the collision system was sufficient to ensure convergence with the number of partial waves for all results presented below.

III. EXPERIMENTAL SETUP

The experimental setup and the details of the measurements are similar to those used by Meintrup *et al.* [30] and Holtkötter and Hanne [31]. Additionally, a new oven for metal vaporization and a movable shutter for the purpose of background correction have been mounted.

In this apparatus, spin-polarized electrons are extracted from a gallium-arsenide (GaAs) crystal, which is irradiated by circularly polarized laser light of wavelength 808 nm. The principle of this spin-polarized electron source was described by Pierce *et al.* [32]. The emitted electron beam is bent by a 90°-deflector and guided by an electrostatic lens system to the collision center where the transversally polarized electrons hit the heavy metal vapor emanating from the oven. A rotatable Jost-type 180° spectrometer [33] is used to collect the scattered electrons. Behind the exit aperture, they are detected by a channel electron multiplier. The primary spin polarization of $P_y = (26.3 \pm 0.6)\%$ was determined by a conventional Mott-type electron polarimeter at 120 keV kinetic energy.

A simplified term scheme of Pb is shown in Fig. 2 for levels up to 4.5 eV. The incident-electron energy was calibrated by observing the impact excitation of the $[\mathrm{Hg}]6p7s\ ^3P_1 \rightarrow [\mathrm{Hg}]6p^2\ ^3P_2$, (405.7 nm) transition using a photomultiplier-filter-lens combination mounted in the scattering plane. A measurement of the excitation function is exhibited in Fig. 3. It shows that the threshold of the transition can be determined with an accuracy of approximately $\Delta E_0 = \pm 0.1$ eV.

The angular resolution $\Delta\vartheta = \pm 2.5°$ of the setup was determined by moving the spectrometer across the 0° direction while the electron beam was attenuated without change to the electron-optical image. The resulting angular distribution has a Gaussian shape. Hence, the FWHM is taken as the angular resolution. From an electron energy-loss spectrum (EELS), the overall energy resolution of $\Delta E = \pm 250$ meV can be estimated from the FWHM of the elastic peak where

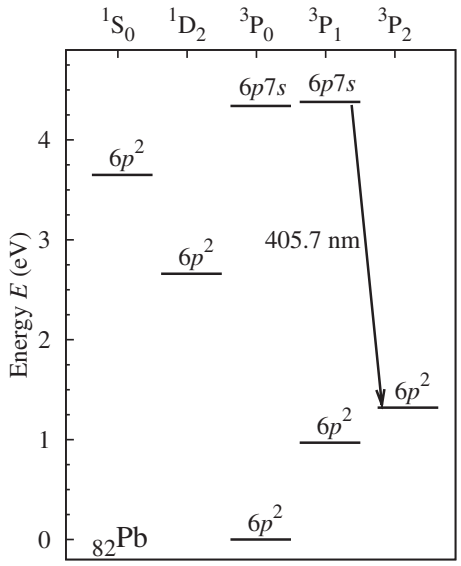

FIG. 2. Energy level diagram of Pb up to 4.5 eV. The labels follow the Russell-Saunders notation. The ground state is $[\mathrm{Hg}]6p^2\ ^3P_0$. The marked transition is used for energy calibration. The levels are taken from [34].

the energy width of the incident electron beam is less than 200 meV.

IV. RESULTS AND DISCUSSION

In Figs. 4 and 5, the earlier [7] and the present results for the spin-asymmetry function between 11 and 14 eV are exhibited in intervals of 0.5 eV. The particular incident energy is indicated in the individual panels. The error bars are determined by the statistical uncertainties.

Generally, the spin-asymmetry function depends strongly on the incident energy in this region. From our measurements it can be seen that two extrema become more and more distinct: a minimum around $\vartheta \approx 85°$ and a maximum near $\vartheta = 105°$. Our results generally agree well with those of Geesmann *et al.* [7] at 11 and 14 eV within the specified uncertainties. Small deviations are observed for the angular range $100 \leq \vartheta \leq 110°$. The angular range of the experimental results was extended to 135° in the present work.

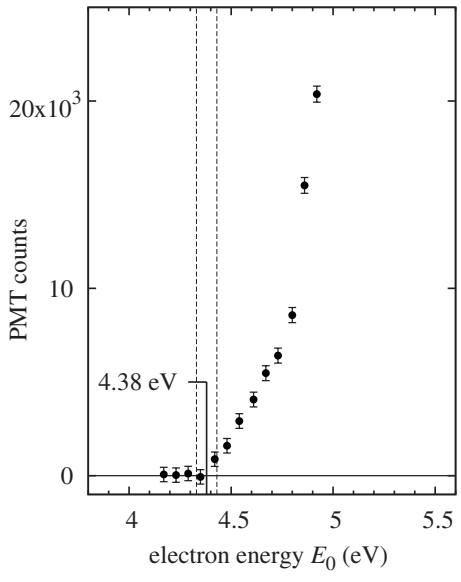

FIG. 3. Energy calibration through the excitation of the transition $6p7s\ ^3P_1 \rightarrow 6p^2\ ^3P_2$ (405.7 nm). The dashed lines indicate the accuracy of the calibration: $\Delta E_0 = \pm 0.1$ eV.

The GKS calculations by Haberland and Fritsche [8] show discrepancies for 11 eV, but they agree well with the experimental data at 14 eV incident energy. These calculations were discussed in detail by Geesmann *et al.* [7].

As can be seen from Fig. 4, the RMP-HF and RMP-DF calculations agree within the error bars for $\vartheta \leq 90°$ for all energies. For 13.5 and 14 eV, the RMP results reproduce the measurements well, even for larger angles. The minimum at $\vartheta \approx 85°$ and the maximum at $\vartheta = 105°$ are also reproduced by these calculations. A steep drop beyond 110° is not supported by the measurements to the extent calculated. Generally, the results of the Hartree-Fock calculations are similar to those of the Dirac-Fock method. Deviations from each other are stronger around 12.5 and 13.0 eV. In this particular case, the RMP-HF model is in slightly better agreement with the experiment. We recall, however, that the present experimental data were used to optimize the parameter β and the radius r_c of the polarization potential through a fitting procedure. Consequently, any conclusion drawn from agreement with experiment, or lack thereof, needs to be viewed in light of this adjustment.

Moving on to Fig. 5, we see that the DBSR-20cc results agree very well with the experimental data. The only noteworthy systematic discrepancy concerns the measured increase in S_A and the corresponding zero crossing around scattering angles of 100° for 13.5 and 14.0 eV incident energy. In the DBSR-20cc results, this structure is shifted by approximately 10° to smaller angles. The RMBP-5cc results, on the other hand, exhibit at best a qualitative agreement with the experimental data. The minimum-maximum structure in the angular dependence of the asymmetry function is generally overestimated by this model. In light of the other results presented here, it is very likely that these problems are mostly due to the lack of accounting for the target polarizability.

V. SUMMARY AND CONCLUSIONS

We have presented experimental data for the spin-asymmetry function S_A measured in elastic scattering of spin-polarized electrons from lead atoms in their $6s^2 6p^2\ ^3P_0$ ground state. A significant energy dependence of the data was found in the energy range 11–14 eV, which may be due, at least in part, to the occurrence of autoionizing states in this particular energy regime.

Comparison with results from various theoretical models shows very satisfactory agreement between experiment and those from a fully relativistic 20-state *B*-spline *R*-matrix (close-coupling) model, which accounts for channel coupling, relativistic effects, possible angular-momentum orientation through resolving the fine structure of the target states,

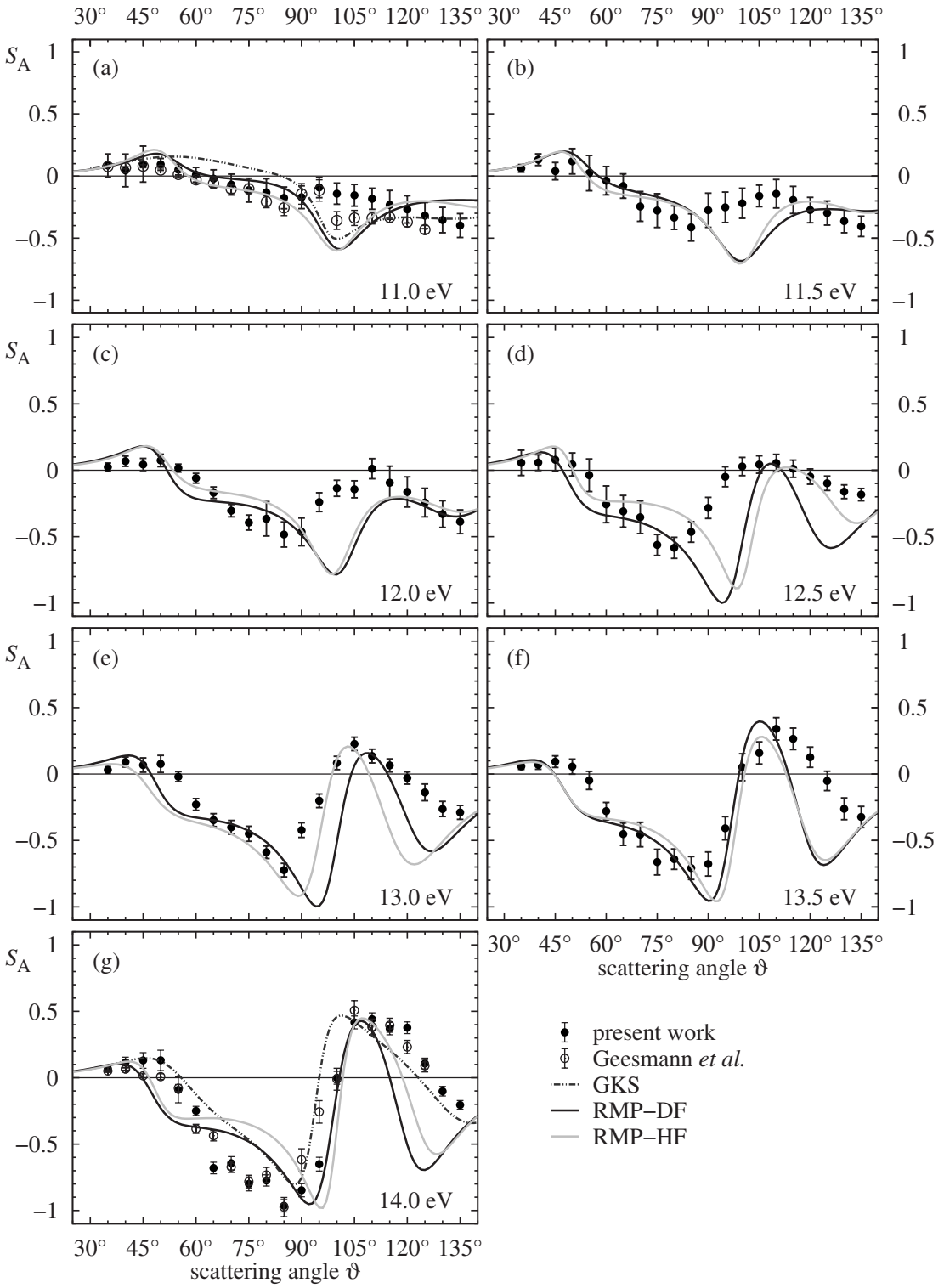

FIG. 4. Spin-asymmetry function S_A for elastic electron scattering from lead atoms at incident energies from 11.0 (a) to 14.0 eV (g) in intervals of 0.5 eV. The present experimental data are compared to those of Geesmann *et al.* [7] and to theoretical results from GKS [8] and the present RMP calculations.

and the influence of autoionizing states. On the other hand, only qualitative agreement with experiment was achieved by a much simpler five-state Breit-Pauli *R*-matrix approach. A single-channel fully relativistic model-potential approach, including local polarization, exchange, and absorption potentials, also performs reasonably well in reproducing the experimental data after adjusting parameters in the polarization potential. Finally, an earlier generalized Kohn-Sham approach, which accounts for polarization and exchange effects in an *ab initio* manner, agrees well with the experimental

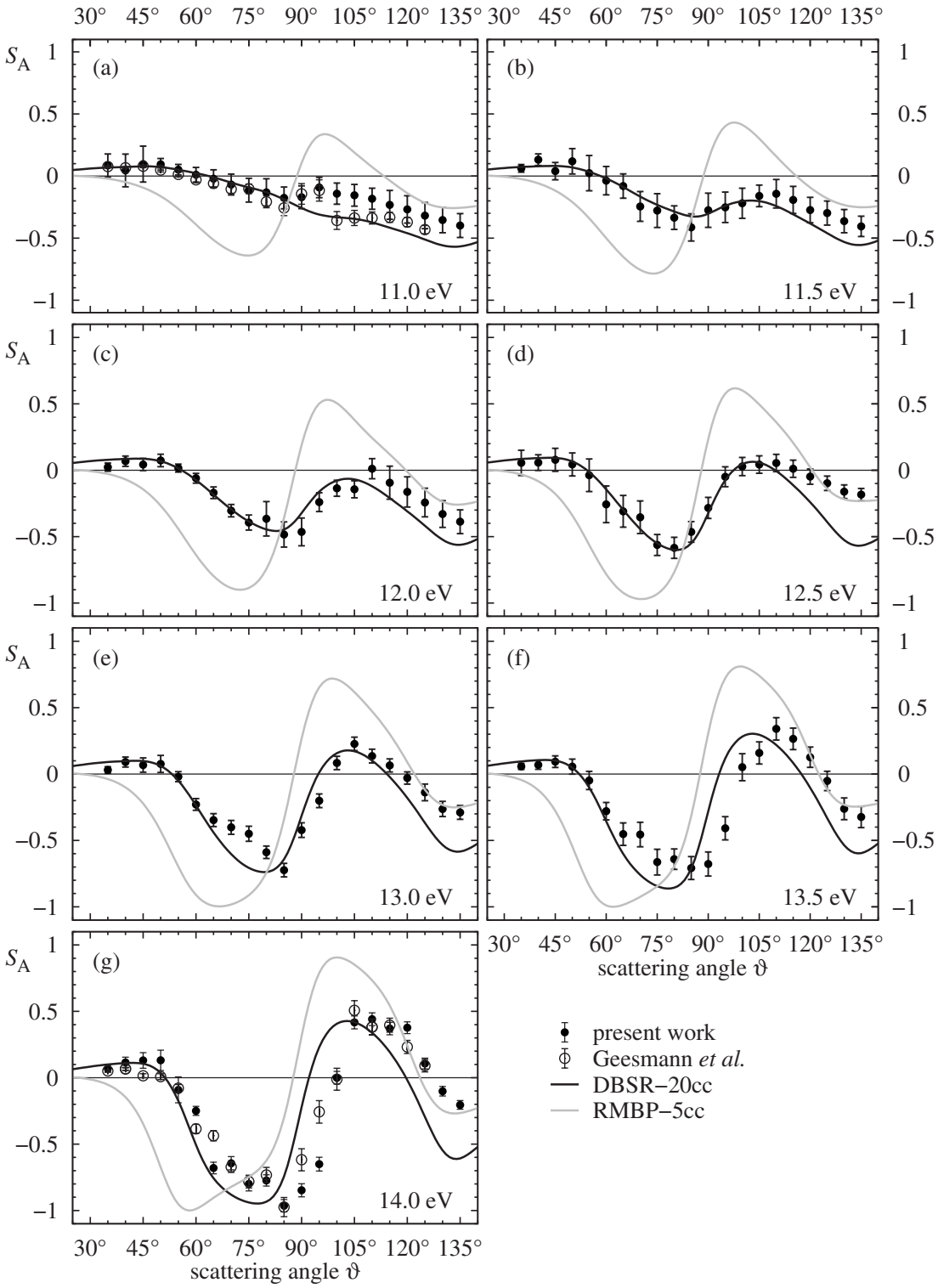

FIG. 5. Spin-asymmetry function S_A for elastic electron scattering from lead atoms at incident energies from 11.0 (a) to 14.0 eV (g) in intervals of 0.5 eV. The present experimental data are compared to those of Geesmann *et al.* [7] and to theoretical results from the present BPRM-5cc and DBSR-20cc calculations.

data at 14 eV, but not so well at 11 eV, thereby indicating a possible direct (through loss of flux) importance of the autoionizing states in this energy regime.

These findings suggest that the outcome of the elastic-scattering processes investigated here is predominantly determined by the electrostatic potential of the target, modified by relativistic, polarization, and exchange effects. Nevertheless, angular-momentum orientation and coupling to autoionizing states should be included in a numerical model to improve the quantitative agreement between theory and experiment. It

will be interesting to see how well the DBSR-20cc model performs for inelastic processes. Describing these transitions is beyond the capabilities of the current GKS and RMP models, and we recall that the BPRM-5cc model was clearly insufficient for these cases. Work in this direction is currently in progress.

ACKNOWLEDGMENTS

This work was supported, in part, by the United States National Science Foundations under Grants No. PHY-0757755 and No. PHY-0903818 (OZ, KB). R.S. and R.K.G. are thankful to Council of Scientific and Industrial Research (CSIR), New Delhi for financial support.

[1] J. Kessler, *Polarized Electrons*, 2nd ed. (Springer-Verlag, New York, Heidelberg, Berlin, Tokyo, 1985).
[2] N. Andersen, K. Bartschat, J. T. Broad, and I. V. Hertel, Phys. Rep. **279**, 251 (1997).
[3] N. Andersen and K. Bartschat, *Polarization, Alignment, and Orientation in Atomic Collisions* (Springer-Verlag, New York, 2001).
[4] M. Dummler, M. Bartsch, H. Geesmann, G. F. Hanne, and J. Kessler, J. Phys. B **25**, 4281 (1992).
[5] G. F. Hanne, Phys. Rep. **95**, 95 (1983).
[6] F. Kaussen, H. Geesmann, G. F. Hanne, and J. Kessler, J. Phys. B **20**, 151 (1987).
[7] H. Geesmann, M. Bartsch, G. F. Hanne, and J. Kessler, J. Phys. B **24**, 2817 (1991).
[8] R. Haberland and L. Fritsche, J. Phys. B **20**, 121 (1987).
[9] K. Bartschat, Phys. Rep. **180**, 1 (1989).
[10] S. D. Tošić, M. S. Rabasović, D. Šević, V. Pejčev, D. M. Filipović, L. Sharma, A. N. Tripathi, R. Srivastava, and B. P. Marinković, Phys. Rev. A **77**, 012725 (2008).
[11] F. A. Parpia, C. Froese Fischer, and I. P. Grant, Comput. Phys. Commun. **94**, 249 (1996).
[12] A. D. McLean and R. S. McLean, At. Data Nucl. Data Tables **26**, 197 (1981).
[13] F. A. Gianturco and S. Scialla, J. Phys. B **20**, 3171 (1987).
[14] G. Staszewska, D. W. Schwenke, and D. G. Truhlar, Phys. Rev. A **29**, 3078 (1984).
[15] S. Milisavljević, D. Šević, R. K. Chauhan, V. Pejčev, D. M. Filipović, R. Srivastava, and P. Marinković, J. Phys. B **38**, 2371 (2005).
[16] M. Adibzadeh and C. E. Theodosiou, Phys. Rev. A **70**, 052704 (2004).
[17] F. Salvat, Phys. Rev. A **68**, 012708 (2003).
[18] K. Bartschat, J. Phys. B **18**, 2519 (1985).
[19] W. Eissner, M. Jones, and H. Nussbaumer, Comput. Phys. Commun. **8**, 270 (1974).
[20] K. A. Berrington, W. Eissner, and P. H. Norrington, Comput. Phys. Commun. **92**, 290 (1995).
[21] V. M. Burke and C. J. Noble, Comput. Phys. Commun. **85**, 471 (1995).
[22] A. N. Grum-Grzhimailo, Comput. Phys. Commun. **152**, 101 (2003).
[23] O. Zatsarinny, Comput. Phys. Commun. **174**, 273 (2006).
[24] O. Zatsarinny and K. Bartschat, Phys. Rev. A **77**, 062701 (2008).
[25] M. Maslov, M. J. Brunger, P. J. O. Teubner, O. Zatsarinny, K. Bartschat, D. V. Fursa, I. B. I, and R. P. McEachran, Phys. Rev. A **77**, 062711 (2008).
[26] O. Zatsarinny, K. Bartschat, M. Maslov, M. J. Brunger, and P. J. O. Teubner, Phys. Rev. A **78**, 042713 (2008).
[27] F. Jüttemann, G. F. Hanne, O. Zatsarinny, and K. Bartschat, Phys. Rev. A **79**, 042712 (2009).
[28] O. Zatsarinny and K. Bartschat, Phys. Rev. A **79**, 042713 (2009).
[29] P. Jönsson, X. He, C. Froese Fischer, and I. P. Grant, Comput. Phys. Commun. **177**, 597 (2007).
[30] R. Meintrup, G. F. Hanne, and K. Bartschat, J. Phys. B **33**, L289 (2000).
[31] I. Holtkötter and G. F. Hanne, Phys. Rev. A **80**, 022709 (2009).
[32] D. T. Pierce and F. Meier, Phys. Rev. B **13**, 5484 (1976).
[33] K. Jost, J. Phys. E **12**, 1006 (1979).
[34] Y. Ralchenko, A. Kramida, J. Reader, and N. A. Team, Nist Atomic Spectra Database (version 3.1.5) (National Institute of Standards and Technology, Gaithersburg, MD, 2008), available at http://physics.nist.gov/asd3